

Evaluation of Meteorological Data-Based Models for Potential and Actual Evapotranspiration Losses Using Flux Measurements

Mirka Mobilia(✉) and Antonia Longobardi

University of Salerno, Via Giovanni Paolo II 132, 84084 Fisciano, Italy
lncs@springer.com

Abstract. Evapotranspiration is a key process within the hydrological cycle, so it requires an accurate assessment. This work aims at assessing monthly scale performances of six meteorological data-based methods to predict evapotranspiration by comparing model estimates with observations from six flux tower sites differing for land cover and climate. Three of the proposed methodologies use a potential evapotranspiration approach (Penman, Priestley-Taylor and Blaney-Criddle models) while the additional three an actual evapotranspiration approach (the Advection-Aridity, the Granger and Gray and the Antecedent Precipation Index method). The results show that models efficiency varies from site to site, even though land cover and climate features appear to have some influence. It is difficult to comment on a general accuracy, but an overall moderate better performance of the Advection-Aridity model can be reported within a context where model calibration is not accounted for. If model calibration is further taken into consideration, the Granger and Gray model appears the best performing method but, at the same time, it is also the approach which is mostly affected by the calibration process, and therefore less suited to evapotranspiration prediction tools dealing with a data scarcity context.

Keywords: Actual evapotranspiration · Potential evapotranspiration · Ameriflux · Fluxnet · Tereno earth observation

1 Introduction

Evapotranspiration (ET) is a key process within the hydrological cycle [1, 2]. It represents a critical parameter in many different applied hydrology studies [3] and uncertainties in its assessment propagate through the hydrological soil-water balance. For this reason, a correct assessment of ET is essential. Eddy covariance (EC) towers represent the best available techniques for determining the ET fluxes but they are expensive to establish and maintain. For these reasons, in the past, many authors have introduced various data-based approaches for actual (AET) and potential (PET) ET modeling [4–6]. Meteorological data-based models for potential evapotranspiration estimation include radiation-based and temperature-based approaches. Among the first type of approaches, the Priestley

© Springer Nature Switzerland AG 2020
O. Gervasi et al. (Eds.): ICCSA 2020, LNCS 12253, pp. 3–18, 2020.
https://doi.org/10.1007/978-3-030-58814-4_1

and Taylor (PT) [7], Turc (TRC) [8], and Abtew (AB) [9] methods are the most common. Among the temperature-based methods, Hargreaves (H) [10], Thornthwaite (TW) [11], Blaney- Criddle (BC) [12] and Linacre (LN) [13] formulations can be listed. The first category requires the solar radiation as the main meteorological variable for the simulation while the second class uses the temperature. A third category is represented by the combination of the previous methods, which couples energetic components, such as net radiation and air temperature, with atmospheric drivers, including air humidity and wind speed. Among these, the Penman (P) model [14, 15] is a universally accepted approach to evaluate potential ET. Concerning actual evapotranspiration, one of the best-known approaches within the class of meteorological data-based methods is the Antecedent Precipitation Index (API) model [16]. Actual evapotranspiration data driven models also include complementary models among which the Advection-Aridity (AA) model [17], the Granger and Gray (GG) model [18], the Complementary Relationship Areal Evaporation (CRAE) model [19], and the modified Advection-Aridity (MAA) model [20]. Considering the large number of proposed approaches, the choice of the most appropriate method for simulating evapotranspiration fluxes is an important issue to be addressed so, in time, many researchers have performed detailed comparative studies [21]. The overall results of the comparative studies suggested that there is not a single approach able to outperform other modeling methods for a particular biome. Given these premises, practical and scientific interest and continuation in this direction appear then encouraged. Within this framework, the current paper presents a comparative analysis where six models and six experimental sites have been taken into consideration. PT, P and BC formulations have been considered for the assessment of potential evapotranspiration, while the AA model, the GG approach and the API model have been considered among actual evapotranspiration empirical relationships. Six experimental sites, belonging to the AMERIFLUX, FLUXNET, and TERENO platforms, have been selected as case studies. They differ in terms of climate type, specifically temperate Oceanic and Mediterranean, and in terms of land covers, specifically forests (FOR), grasslands (GRA) and croplands (CRO). Testing and comparing the performance of the six models for the six experimental sites, it was possible to provide recommendations about the most suited method to be applied in the case of a calibrated and non-calibrated approach and furthermore it was possible to identify, for each model, which is the importance and impact generated by the calibration itself.

2 Materials and Methods

2.1 The Case Studies

Experimental data have been used to compare the relative performance of the selected approaches for evapotranspiration assessment. Six EC towers have been selected for this purpose, belonging to the TERENO (http://teodoor.icg.kfa-juelich.de/overview-en), FLUXNET (http://fluxnet.fluxdata.org/), and AMERIFLUX global networks (http://ameriflux.lbl.gov/). They are representative of specific biomes as they focus on the combination of three different land covers which are grassland, cropland and forests and two climatic regions namely the Mediterranean and the Oceanic climate. According to the Koppen classification [22], the Mediterranean climate (Cs) is characterized by hot, dry

summers and cool, wet winters with the highest percentage of rain in the year. The Mediterranean climate includes the subtypes "Csa" and "Csb" where the letter "a" represents an average temperature in the warmest month above 22 C, while "b" indicates the average temperature in the warmest month below 22 C. The oceanic climate (Cf) has cool but not cold winters and warm summers, precipitation is evenly distributed throughout the year. Cf splits in "Cfa" and "Cfb" too. Six sites with the selected biomes have been analyzed in the present research including "us-twt" in California, "us-arm" in Oklahoma, "us-fwf" located in Arizona, "de-rur" and "de-hai" in Germany, "us-me3" in Oregon. Figure 1 shows the location of the stations, the identification number (ID) and the corresponding platforms.

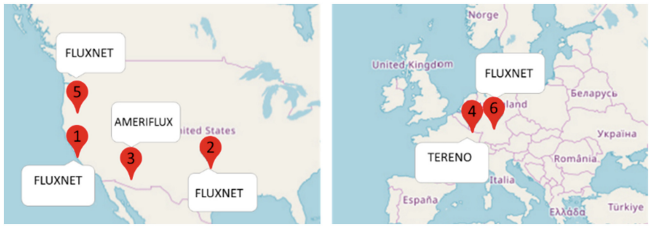

Fig. 1. Location of the investigated flux towers in U.S.A. and Europe.

As an additional climate characterization, which will help the discussion of the results, the moisture index (IM) has been estimated. The moisture index [11], previously calculated for the six sites, allows to classify the climate conditions of various geographical areas. Table 1 represents climate types together with the range of their IM values:

Table 1. Thornthwaite's climate types according to moisture index I_M.

Climatic Type	I_M
Per Humid	>100
B4) Humid (Strongly)	from 81 to 100
B3) Humid	from 61 to 80
B2) Humid (Moderate)	from 41 to 60
B1) Humid (Mild)	from 21 to 40
C2) Moist Sub-humid	from 0 to 20
C1) Dry Sub-humid	from −20 to 0
D) Semi-arid	from −40 to −21
E) Arid	from −60 to −41

Additional details for each site are listed in Table 2, including relevant references and Thornthwaite moisture index (IM).

Table 2. Experimental sites and their main characteristics

ID	Name	Vegetation type	Record period	Climate	Mean annual temperature (°C)	Mean annual Precipitation (mm)	IM (−)	References
1	us-twt	CRO	2009 to 2014	CSA	14.6	344	−65	[23]
2	us-arm	CRO	2003 to 2012	CFA	15.3	646	−40	[24]
3	us-fwf	GRA	2006 to 2012	CSB	8.4	539	−7	[25]
4	de-rur	GRA	2012 to 2017	CFB	8.4	895	68	[26]
5	us-me3	FOR	2004 to 2009	CSB	8.2	384	−30	[27]
6	de-hai	FOR	2000 to 2007	CFB	8.3	806	47	[28]

2.2 Model Description and Evaluation

Estimates from six models have been compared with observational data. Three potential evapotranspiration models and three actual evapotranspiration models have been selected. They are briefly described in the following.

Potential Evapotranspiration Approaches. In order to model baseline PET, Penman (P) equation known as a combination-type technique, Priestley–Taylor (PT) method among the radiation-based models and Blaney–Criddle (BC) equation belonging to the class of temperature-based approaches, have been proposed. Penman (P) formulation can be written as:

$$PET_P = \frac{1}{\lambda}\left[\frac{\Delta}{\Delta+\gamma}(R_n - G_{soil})\right] + \left[\frac{\gamma}{\gamma+\Delta}E_A\right] \tag{1}$$

where Δ is the slope of the saturation vapor pressure–temperature curve (kPa $°C^{-1}$), γ represents the psychrometric constant (kPa $°C^{-1}$), λ represents the latent heat of vaporization (MJ kg^{-1}), and E_A represents the drying power of the air, which is expressed as:

$$E_A = 2.6(1 + 0.54u)(e_s - e_a) \tag{2}$$

where u represents the wind speed (ms^{-1}), $2.6(1 + 0.54{\cdot}u)$ is the wind function f(u), e_s represents the saturation vapor pressure (kPa), e_a represents the vapor pressure (kPa), Rn represents the net radiation (MJ m^{-2} d^{-1}) and G_{soil} represents the soil heat-flux density at the soil surface (MJ m^{-2} d^{-1}).

Priestley–Taylor formulation is given as:

$$PET_{PT} = \frac{1}{\lambda} \cdot \alpha \left[\frac{\Delta}{\Delta + \gamma} (R_n - G_{soil}) \right] \tag{3}$$

where α represents the advection correction coefficient, with a value of 1.26.

The usual form of the Blaney-Criddle equation is:

$$PET_{BC} = \mathrm{k}p(0.46 \cdot T_{mean} + 8) \tag{4}$$

where p is the percentage of total daytime hours for the considered period (daily or monthly) out of total daytime hours of the year, k is the monthly consumptive use coefficient.

Actual Evapotranspiration Approaches. Three meteorological data-based models have been used to quantify actual evapotranspiration losses: the AA-model, the GG model and the API model. The Advection-Aridity model, the Granger and Gray model are two of the most broadly used approaches among the class of complementary relationship (CR). Actual evapotranspiration derived by the AA method results from Eq. (5):

$$AET_{AA} = (2\alpha - 1)\frac{1}{\lambda}\left[\frac{\Delta}{\Delta + \gamma} (R_n - G_{soil}) \right] - \left[\frac{\gamma}{\gamma + \Delta} E_A \right] \tag{5}$$

According to the GG model, actual evapotranspiration can be estimated instead as follows:

$$AET_{GG} = \left[\frac{\Delta \cdot G}{\Delta + \gamma} \left(\frac{R_n - G_{soil}}{\lambda} \right) \right] + \left[\frac{\gamma \cdot G}{\gamma + \Delta \cdot G} E_A \right] \tag{6}$$

where G is the relative evaporation parameter expressed as:

$$G = \frac{1}{0.793 + 0.20e^{4.902D}} + 0.006D \tag{7}$$

In the previous equation, D is the relative drying power:

$$D = \frac{E_A}{E_A + R_n} \tag{8}$$

The third model selected in the present analysis for estimating actual evapotranspiration is the API model. According to this model, the actual evapotranspiration rates are expressed as:

$$AET_{API} = \frac{1}{\lambda} \cdot \alpha_{API} \left[\frac{\Delta}{\Delta + \gamma} (R_n - G_{soil}) \right] \tag{9}$$

The dimensionless coefficient, α_{API}, is expressed as a threshold function of the Antecedent precipitation index (API). Given a threshold value of the API equal to 20 mm, if the current API value is lower than or equal to the threshold API, then:

$$\alpha_{API} = 0.123(API) - 0.0029(API)^2 - 0.0000056(API)^3 \tag{10}$$

If the current API value is larger than the threshold API, then:

$$\alpha_{API} = 1.26 \tag{11}$$

API is given by the following formula:

$$API = \sum_{t=-1}^{-i} P_t k^{-t} \tag{12}$$

where i represents the considered number of antecedent days, k represents the decay constant, and P_t represents rainfall during day t.

Models Evaluation. Monthly scale ET losses modeled using the above described meteorological data-based approaches are in the following compared to the observed ET fluxes from the EC measurements, for purpose of model evaluation. The comparison will help to test the ability of the models to predict actual evapotranspiration fluxes but, even more importantly, it helps to detect the limitations of each approach. For an overall model evaluation, three goodness-of-fit statistics have been accounted for. These are the normalized root mean square error (RMSEd) as a measure of error intensity, the index of agreement (d) as a measure of patterns agreement, the correlation coefficient (r) as a measure of correlation between observed and modelled variables. They are estimated as follows:

$$RMSE(mm) = \left[\frac{1}{n}\sum_{i=1}^{n}\left(ET_{mod,i} - ET_{EC,i}\right)^2\right]^{\frac{1}{2}} \tag{13}$$

$$RMSEd(-) = \frac{RMSE(mm)}{\overline{ET}_{EC}} \tag{14}$$

$$d(-) = 1 - \frac{\sum_{i=1}^{n}\left|ET_{mod,i} - ET_{EC,i}\right|}{\sum_{i=1}^{n}\left(\left|ET_{mod,i} - \overline{ET}_{EC,i}\right| + \left|ET_{obs,i} - \overline{ET}_{EC,i}\right|\right)} \tag{15}$$

$$r(-) = \frac{Cov(ET_{mod}, ET_{EC})}{\sigma(ET_{mod})\sigma(ET_{EC})} \tag{16}$$

where n represents the length of the monthly sample, $ET_{mod,i}$ and $ET_{EC,i}$ respectively represent the monthly values of the modeled and the observed (i.e., derived from EC fluxes) evapotranspiration fluxes, and σ is the ET standard deviation.

3 Results

3.1 Monthly AET Prediction Models Results

Although all the six models present similar temporal ET patterns, substantial differences in the magnitude of evapotranspiration water losses exist among them, with an exception for one site (de-rur ID4). At a first visual inspection (Fig. 2), all methods appear to overestimate the ET_{EC} measurements but for a quantitative assessment of models' performances in predicting monthly scale ET losses, the goodness-of-fit indices evaluation is reported in Table 3. Furthermore, Fig. 3 illustrates the goodness-of-fit indices for the best performing method for each experimental site.

Table 3. Goodness of fit indices for the different models and experimental sites. In bold the best-performing methods for each site.

Site	Models	RMSEd(−)	d(−)	r(−)	Site	Models	RMSEd(−)	d(−)	r(−)
us-twt (CRO- Csa) ID1	API	0.42	0.73	0.83	de-rur (GRA-Cfb) ID4	API	0.18	0.89	0.99
	AA	0.43	0.69	0.80		AA	0.29	0.80	0.97
	GG	0.29	0.81	0.91		GG	0.21	0.87	0.99
	P	0.67	0.63	0.87		P	0.41	0.74	0.99
	PT	0.26	0.82	0.93		PT	0.20	0.88	0.99
	Blaney-Criddle	0.54	0.57	0.91		Blaney-Criddle	1.23	0.33	0.98
us-arm (CRO- Cfa) ID2	API	1.24	0.47	0.69	us-me3 (FOR- Csb) ID5	API	1.94	0.37	0.75
	AA	0.67	0.57	0.70		AA	1.28	0.49	0.79
	GG	1.12	0.49	0.71		GG	1.97	0.35	0.72
	P	2.54	0.18	0.58		P	2.78	0.24	0.66
	PT	1.24	0.47	0.69		PT	1.99	0.36	0.72
	Blaney-Criddle	2.21	0.19	0.61		Blaney-Criddle	2.67	0.19	0.73
us-fwf (GRA- Csb) ID3	API	0.95	0.55	0.82	de-hai (FOR- Cfb) ID6	API	1.34	0.59	0.96
	AA	0.63	0.54	0.85		AA	0.81	0.75	0.94
	GG	1.21	0.48	0.77		GG	1.41	0.56	0.95
	P	2.68	0.19	0.70		P	2.05	0.38	0.95
	PT	0.97	0.53	0.81		PT	1.34	0.59	0.96
	Blaney-Criddle	2.05	0.22	0.83		Blaney-Criddle	3.43	0.20	0.96

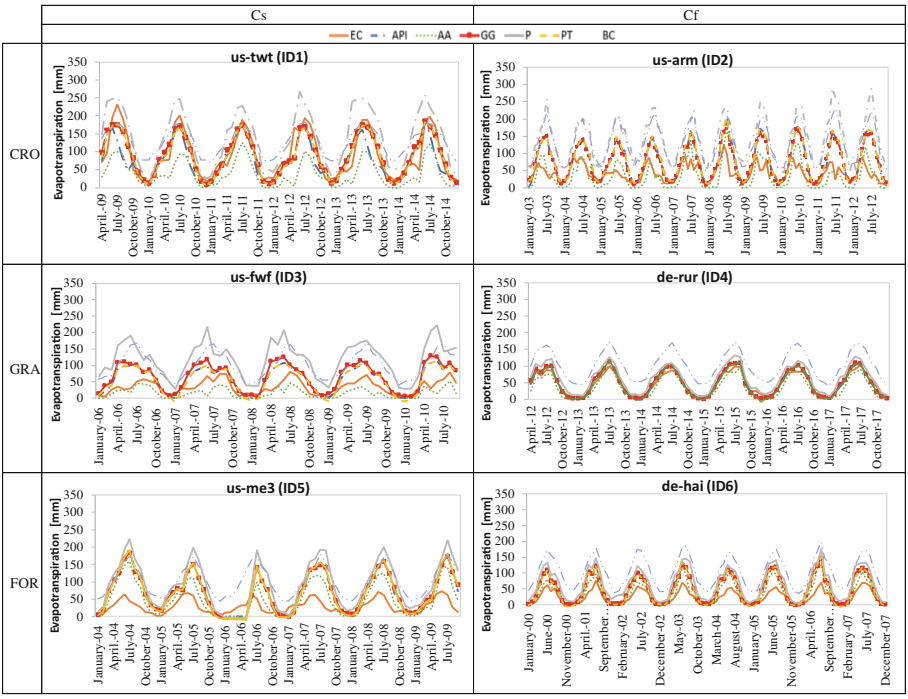

Fig. 2. Monthly patterns of observed and modelled evapotranspiration by using API, AA, GG, PM, PT, BC methods

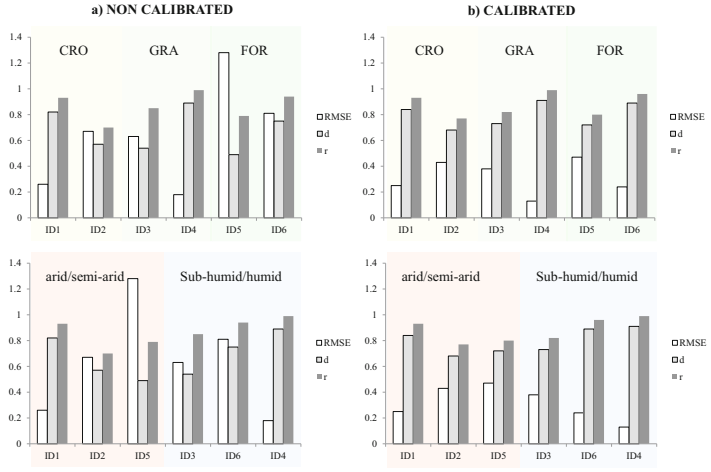

Fig. 3. GOF statistics for the best performing method for each site in the case of a) non calibrated approach and b) calibrated approach with reference to land cover and moisture index IM

The results underline the following key issues:

1. Overall and evidently the PET models result the worst-performing since they return the largest ET overestimation.
2. Among PET approaches, PT-model represents an exception to the rule as it is not only the best performing among PET models but also presents a fitting comparable to AET prediction methods (in particular to the API method). In addition, for the site us-twt (ID1), the Priestley-Taylor approach has been found to be the best performing method;
3. AET models are better able to predict ET rather than the PET ones. Among these, AA approach appears to be characterized by the lowest errors in most of the investigated cases (ID 2, 6, 3, 5) and comparable in the remaining (ID 1, 4).
4. The use of Antecedent Precipitation Index approach better describes the monthly scale evapotranspiration demands in only one case (ID4). Anyway, it should be considered that, for this particular site, the errors associated to all AET methods are comparable with each other.
5. Forest cover type systems (ID5 and ID6) seem associated to the largest prediction errors (larger RMSE and lower r and d) over the studied sites (Fig. 3 upper right panel);
6. Regardless for the land cover type, systems ID3, ID4 and ID6 featured by humid and sub-humid climate conditions seem associated to the lowest prediction errors (lowest RMSE and largest r and d) as illustrated in Fig. 3 lower right panel;
7. Finally, ET values result generally overestimated by all the models with significant percentages error (on average RMSE = 64%). This evidence points to the need to use a calibration procedure to improve meteorological data-based modeling of ET processes as described in the following paragraph.

3.2 AET Models Calibration

The previous analysis has shown large model uncertainties in ET assessment. Possible explanation for the significant errors can be found in the lack of a site-specific calibration of the model parameters so, in order to optimize the evapotranspiration estimates, the calibration of such parameters has been further introduced. As a confirmation of this, many authors in the past have argued about the need for the calibration of the model parameters in order to improve ET prediction [29]. In this study, the calibration process has concerned only the AET models since they have been proven to better perform than the PET ones. The parameters subject to the calibration are the wind function f(u) (for the AA method), the relative evaporation parameter G (for the GG method) and the α-coefficient (for both the API and the AA methods). A moderate range of variability has been reported for such parameters in the relevant literature. Concerning the PT proportionality constant, the proposed values range between 1.05 and 2.20 [30, 31]. As regard to the wind function, there have been many studies dealing with this issue that suggested $a_w = 0.37$ and $b_w = 0.22$ [32], or $a_w = 1.313$ and $b_w = 1.381$ [33] or $a_w = 0.1954$ and $b_w = 0.4703$ [34]. With reference to G, this parameter was empirically derived from several authors [35]. In the current study, the API and the GG approaches have been calibrated in a one-step approach (compared to the AA as later described) where,

at the monthly scale, the best match between the eddy covariance ET (ET_{EC}) and the observed data has been achieved minimizing model errors. The calibrated formulations of the relative evaporation, G_{CAL}, and the calibrated Priestley-Taylor coefficient α_{CAL} resulting from this calibration process, has been shown in Table 4. The calibration of AA model consists of two phases [36] since it presents a two-terms structure. For the calibration of the term linked to the drying power of advected air, only the data from the moist days have been used. Moist days have been identified on the base of soil water content higher than a threshold value of 20% [37]. The wind function has been iteratively calibrated until the measured and modelled values of ET during the well-watered days reach the largest match. In the second step, the calibration of α has been performed for the whole period of observation regardless of dry and wet days. In Table 4, the calibrated wind function and Priestley-Taylor coefficient have been shown for each site. As evident in Table 4, α_{CAL}, for the calibrated API model, is similar to 1.26 in the cases of ID1 and ID4, whereas significantly deviates from it for the remaining cases. In the case of the AA model, α_{CAL} is more likely similar to the 1.26 standard coefficient. The calibrated parameter G, assumes for ID4 and ID6 a formulation similar to the one originally used in GG model, in the other cases, the constants remarkably differ from their non-calibrated values. In the end, as regard to the wind function, the calibration process returns for each site a value of b_w about ten times lower than 0.54 which is the non-calibrated parameter.

Table 4. Goodness of fit indices for the different experimental sites. Comparison is made between calibrated models and the non-calibrated best performing models (Table 3).

Site	Models	RMSEd(−)	d(−)	r(−)	Calibrated parameters
us-twt (CRO-Csa) ID1	API_{cal}	0.25	0.84	0.93	$\alpha_{cal} = 1.33$
	AA_{cal}	0.32	0.81	0.92	$\alpha_{cal} = 1.46$; $f(u)_{cal} = 3.2(1 + 0.029u)$
	GG_{cal}	0.27	0.84	0.92	$G_{cal} = 1/(1.5 + 3 \cdot 10^{(-6)} e^{27.3D}) + 0.044 \cdot D$
	PT	0.26	0.82	0.93	–
us-arm (CRO-Cfa) ID2	API_{cal}	0.48	0.61	0.69	$\alpha_{cal} = 0.57$
	AA_{cal}	0.64	0.50	0.73	$\alpha_{cal} = 1.22$; $f(u)_{cal} = 4.3(1 + 0.02u)$
	GG_{cal}	0.43	0.68	0.77	$G_{cal} = 1/(0.55 + 0.035e^{13.02D}) + 0.061 \cdot D$
	AA	0.67	0.57	0.70	–
us-fwf (GRA-Csb) ID3	API_{cal}	0.38	0.73	0.82	$\alpha_{cal} = 0.77$
	AA_{cal}	0.47	0.71	0.80	$\alpha_{cal} = 1.30$; $f(u)_{cal} = 4.2(1 + 0.012u)$
	GG_{cal}	0.39	0.72	0.80	$G_{cal} = 1/(0.77 + 1.68e^{3.15D}) + (0.0881 \cdot D)$
	AA	0.63	0.54	0.85	–

(*continued*)

Table 4. (*continued*)

Site	Models	RMSEd(−)	d(−)	r(−)	Calibrated parameters
de-rur (GRA-Cfb) ID4	API_{cal}	0.15	0.90	0.99	$\alpha_{cal} = 1.22$
	AA_{cal}	0.21	0.87	0.98	$\alpha_{cal} = 1.25$; $f(u)_{cal} = 2.53(1 + 0.054u)$
	GG_{cal}	0.13	0.91	0.99	$G_{cal} = 1/(1.2 + 0.2e^{4.3D}) + 0.012 \cdot D$
	API	0.18	0.89	0.99	–
us-me3 (FOR-Csb) ID5	API_{cal}	0.59	0.65	0.73	$\alpha_{cal} = 0.57$
	AA_{cal}	0.65	0.64	0.78	$\alpha_{cal} = 0.92$; $f(u)_{cal} = 1.88(1 + 0.0035u)$
	GG_{cal}	0.47	0.72	0.80	$G_{cal} = 1/(3.63 + 0.005e^{22.62D}) + 0.07 \cdot D$
	AA	1.28	0.49	0.79	–
de-hai (FOR-Cfb) ID6	API_{cal}	0.30	0.87	0.96	$\alpha_{cal} = 0.56$
	AA_{cal}	0.42	0.84	0.95	$\alpha_{cal} = 1.03$; $f(u)_{cal} = 3.10(1 + 0.0005u)$
	GG_{cal}	0.24	0.89	0.96	$G_{cal} = 1/(3.93 + 0.395e^{4.09D}) + 0.0069 \cdot D$
	AA	0.81	0.75	0.94	–

The accuracy of the AET values provided by the calibrated models (API_{CAL}, AA_{CAL}, GG_{CAL}), has been tested and compared to that resulting from the best performing model (before calibration process) by using the goodness of fit indices suggested in the paragraph 2.2. Results are illustrated in Table 4. In addition, for comparative purpose, the monthly patterns of modelled evapotranspiration resulting from the same models reported in Table 4, have been shown in Fig. 4. From the monthly patterns illustrated in Fig. 4, as expected, it can be seen that monthly evapotranspiration losses provided by the calibrated approaches appear to be more consistent with the EC measurements, also compared to the best-performing method prior to calibration. This circumstance is also supported by the goodness-of-fit assessment (Table 4) which allows to quantitatively assess whether the local calibration improves the confidence in ET estimates derived from the API, AA and GG models. Similarly, to the case of non-calibrated approaches, systems featured by sub-humid/humid climate conditions (Cfb) seem associated to the lowest prediction errors (Fig. 3 lower right panel) as well as forest cover type seems associated to the largest errors (Fig. 3 upper right panel). Overall, the GG_{cal} model appears the best performing calibrated model, while AA_{cal} is the least accurate model probably because of the complex calibration procedure.

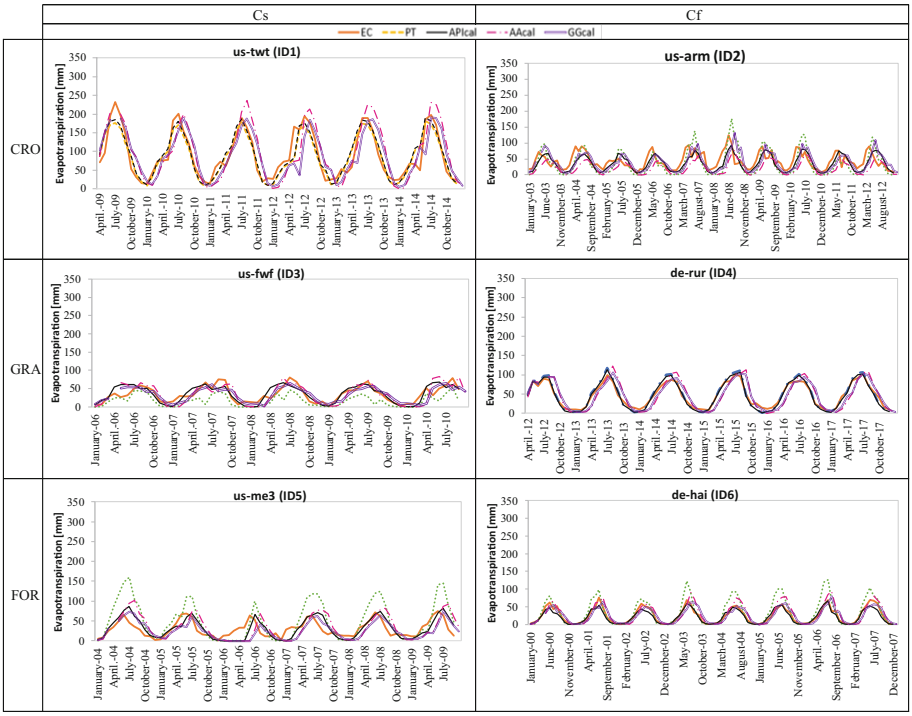

Fig. 4. Monthly patterns of modelled and observed evapotranspiration by using API_{CAL} method compared to the best performing model before calibration process.

The improvement determined by the model parameters calibrated can be better detected with reference to Fig. 5. RMSE, d and r variations are computed as the relative differences between the non-calibrated and the calibrated approaches.

RMSE variations are overall positive, entailing a reduction of RMSE after the calibration for each method and for each site, thus an improvement in model performance. Similarly, d and r variations are overall negative, entailing an increase in d and r after the calibration for each method and for each site, thus an improvement in model performance. Variations in RMSE and d are considerably larger than variations in r, and they are particularly large in the case of the FOR land cover. Among the applied models, the GG which appeared the best performing calibrated model, is the approach most affected by the calibration, with RMSE variation up to 83% and d reduction up to 106%.

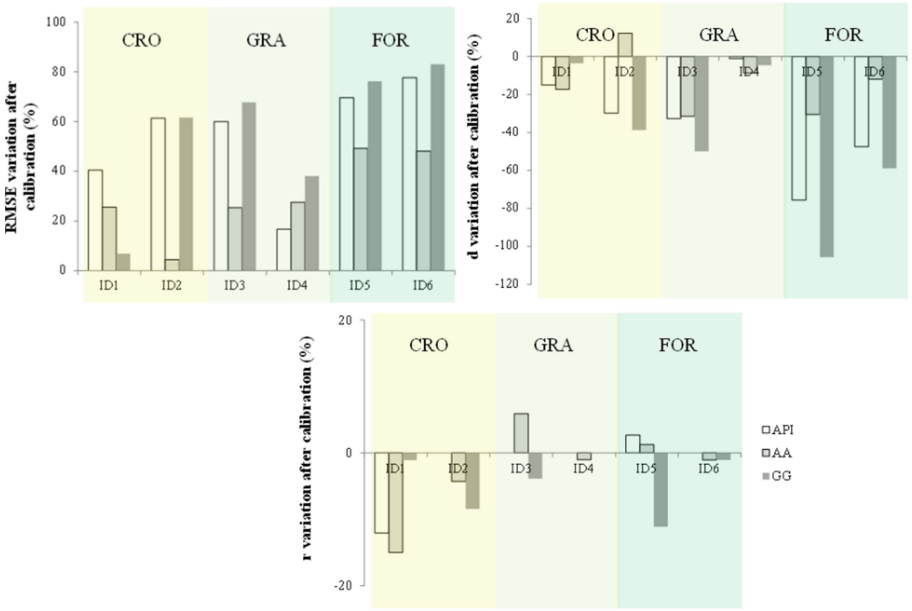

Fig. 5. RMSE, d and r variation caused by model parameters calibration.

4 Conclusion

The performance of six meteorological data-based evapotranspiration models has been evaluated using high-quality dataset of selected eddy covariance towers from FLUXNET, AMERIFLUX and TERENO platforms, characterized by different land covers and climate conditions. AET fluxes have been computed using three models: the GG, the AA and the API models. With regard to the PET approaches, a temperature-based method (i.e. Blaney–Criddle equation), a radiation-based model (Priestley–Taylor methodology) and a combination-type technique (Penman equation) have been tested. Even though it appeared difficult to comment on a general accuracy of the models, varying from site to site, and in finding a single modelling scheme which would be more appropriate for a specific combination of climate and vegetation type, some general tendencies have been detected. AET models have been obviously found to be better in modelling the eddy covariance ET estimates. In a non-calibrated approach, the AA model appeared the best performing method in almost all investigated cases. Systems featured by forest land cover and arid/semi-arid climate conditions have been associated to the largest model errors. Average RMSE, d and r amount to about 64%, 68% and 87%, highlighting the need for a calibration in order to improve model efficiency. Model parameters calibration involved the wind function f(u) for the AA method, the relative evaporation parameter G for the GG method, and the α-coefficient for both the API and the AA methods. Particularly for what concerned the AA method, the calibration process was particularly complex, and all the calibrated parameters significantly deviate from standard coefficients definition. The results of the calibration were obviously an increase in models' efficiency, with average RMSE, d and r that amount to about 32%, 80% and 88% after calibration. Nevertheless,

after the calibration, systems featured by forest land cover and arid/semi-arid climate conditions have been still associated to the largest model errors. A change in the best performing method is clearly visible, with the GG approach that represent the overall best performing in the case of calibration. This circumstance is accompanied by the fact that the GG model is also, among the applied methods, the most affected by the calibration. On the contrary, AA seems to be the least impacted. The results of such a comparative study in contrasting environment could provide suggestions and recommendations for the selection of the best suited methodology to be used for ET predictions to face the lack of data challenge.

Acknowledgments. This work used eddy covariance data acquired and shared by the FLUXNET community, including these networks: AmeriFlux, AfriFlux, AsiaFlux, CarboAfrica, CarboEuropeIP, CarboItaly, CarboMont, ChinaFlux, Fluxnet-Canada, GreenGrass, ICOS, KoFlux, LBA, NECC, OzFlux-TERN, TCOS-Siberia, and USCCC. The ERA-Interim reanalysis data are provided by ECMWF and processed by LSCE. The FLUXNET eddy covariance data processing and harmonization was carried out by the European Fluxes Database Cluster, AmeriFlux Management Project, and Fluxdata project of FLUXNET, with the support of CDIAC and ICOS Ecosystem Thematic Center, and the OzFlux, ChinaFlux and AsiaFlux offices.

The authors also gratefully acknowledge the support of TERENO, funded by the Helmholtz Association, and the SFB-TR32 "Pattern in Soil–Vegetation–Atmosphere Systems: Monitoring, Modeling and Data Assimilation", funded by the Deutsche Forschungsgemeinschaft (DFG).

This research has been supported by the U.S. Department of Energy's Office of Science (Grant No. DE-FG02-06ER64318 and DE-AC02-05CH11231 for the AmeriFlux core site) and the US Department of Energy (Grant DE-SC0012194) and Agriculture and Food Research Initiative of the US Department of Agriculture National Institute of Food and Agriculture (Grants 2013-67003-20652, 2014-67003-22065, and 2014-35100-22066) for our North American Carbon Program studies, "Carbon cycle dynamics within Oregon's urban-suburban-forested-agricultural landscapes".

We would like to thank you for providing data, the Office of Biological and Environmental Research of the US Department of Energy under contract No. DE-AC02-05CH11231 as part of the Atmospheric Radiation Measurement Program (ARM) and California Department of Water Resources; USDA/AFRI Funding for AmeriFlux data resources was provided by the U.S. Department of Energy's Office of Science.

References

1. Longobardi, A., Khaertdinova, E.: Relating soil moisture and air temperature to evapotranspiration fluxes during inter-storm periods at a mediterranean experimental site. J. Arid Land **7**(1), 27–36 (2015)
2. Mobilia, M., Longobardi, A.: Model details, parametrization, and accuracy in daily scale green roof hydrological conceptual simulation. Atmos. **11**(6), 575 (2020)
3. Sartor, J., Mobilia, M., Longobardi, A.: Results and findings from 15 years of sustainable urban storm water management. Int. J. Saf. Sec. En. **8**(4), 505–514 (2018)
4. Makkink, G.F., Van Heemst, H.D.J.: The actual evapotranspiration as a function of the potential evapotranspiration and the soil moisture tension. Njas-wagen J. Life sc. **4**(1), 67–72 (1956)
5. Caprio, J.M.: The solar thermal unit concept in problems related to plant development and potential evapotranspiration. Phenol. Season. Mod. **8**, 353–364 (1974)

6. Bair, W., Robertson, G.W.: A new versatile soil moisture budget. Can. J. Plant Sci. **46**(3), 299–315 (1996)
7. Priestley, C.H.B., Taylor, R.J.: On the assessment of surface heat flux and evaporation using large-scale parameters. Mon. Weather Rev. **100**(2), 81–92 (1972)
8. Turc, L.: Estimation of irrigation water requirements, potential evapotranspiration: a simple climatic formula evolved up to date. Ann. Agron. **12**(1), 13–49 (1961)
9. Abtew, W.: Evapotranspiration measurements and modeling for three wetland systems in south Florida. J. Am. Water Resour. As. **32**(3), 465–473 (1996)
10. Hargreaves, G.: Preciseness of estimated reference crop evapotranspiration. J. Irrig. Drain. Eng. **115**(6), 1000–1007 (1989)
11. Thornthwaite, C.W.: An approach toward a rational classification of climate. Geogr. Rev. **38**, 55–94 (1948)
12. Blaney, H.F., Criddle, W.D.: Determining water requirements in irrigated areas from climatological and irrigation data. Soil Conserv. Serv. **96**, 48 (1950)
13. Linacre, E.T.: A simple formula for estimating evaporation rates in various climates, using temperature data alone. Agric. Meteorol. **18**(6), 409–424 (1977)
14. Penman, H.L.: Natural evaporation from open water, bare soil and grass. Proc. R. Soc. Lond. Series Math. Phys. Sci. **193**(1032), 120–145 (1948)
15. Penman, H.L.: Vegetation and hydrology. Soil Sci. **96**(5), 357 (1963)
16. Marasco, D.E., Culligan, P.J., McGillis, W.R.: Evaluation of common evapotranspiration models based on measurements from two extensive green roofs in New York city. Ecol. Eng. **84**, 451–462 (2015)
17. Mobilia, M., Longobardi, A., Sartor, J.F.: Including a-priori assessment of actual evapotranspiration for green roof daily scale hydrological modelling. Water **9**(2), 72 (2017)
18. Granger, R.J., Gray, D.M.: Evaporation from natural nonsaturated surfaces. J. Hydrol. **111**(1–4), 21–29 (1989)
19. Xu, Z.X., Li, J.Y.: Estimating basin evapotranspiration using distributed hydrologic model. J. Hydrol. Eng. **8**(2), 74–80 (2003)
20. Szilagyi, J., Hobbins, M.T., Jozsa, J.: Modified advection-aridity model of evapotranspiration. J. Hydrol. Eng. **14**(6), 569–574 (2009)
21. Fisher, J.B., Tu, K.P., Baldocchi, D.D.: Global estimates of the land–atmosphere waterflux based on monthly AVHRR and ISLSCP-II data, validated at 16 FLUXNET sites. Remote Sens. Environ. **112**, 901–919 (2008)
22. Köppen, W.: Das geographische System der Klimate. Handbuch der Klimatologie, Borntraeger (1936)
23. Knox, S.H., Matthes, J.H., Sturtevant, C., Oikawa, P.Y., Verfaillie, J., Baldocchi, D.: Biophysical controls on interannual variability in ecosystem-scale CO2 and CH4 exchange in a California rice paddy. J. Geophys. Res. Biogeosci. **121**(3), 978–1001 (2016)
24. Lokupitiya, E., et al.: Incorporation of crop phenology in simple biosphere model (SiBcrop) to improve land-atmosphere carbon exchanges from croplands. Biogeosci. **6**(6), 969–986 (2009)
25. Dore, S., et al.: Recovery of ponderosa pine ecosystem carbon and water fluxes from thinning and stand-replacing fire. Global Change Biol. **18**(10), 3171–3185 (2012)
26. Borchard, N., et al.: Spatio-temporal drivers of soil and ecosystem carbon fluxes at field scale in an upland grassland in Germany. Agric. Ecosyst. Environ. **211**, 84–93 (2015)
27. Kwon, H., Law, B.E., Thomas, C.K., Johnson, B.G.: The influence of hydrological variability on inherent water use efficiency in forests of contrasting composition, age, and precipitation regimes in the Pacific Northwest. Agric. Meteorol. **249**, 488–500 (2018)
28. Rebmann, C., et al.: Quality analysis applied on eddy covariance measurements at complex forest sites using footprint modelling. Theo. Appl. Climatol. **80**(2–4), 121–141 (2005)

29. Tabari, H., Grismer, M.E., Trajkovic, S.: Comparative analysis of 31 reference evapotranspiration methods under humid conditions. Irrig. Sci. **31**(2), 107–117 (2013)
30. McNaughton, K.G., Black, T.A.: A study of evapotranspiration from a Douglas fir forest using the energy balance approach. Water Resour. Res. **9**(6), 1579–1590 (1973)
31. Cristea, N.C., Kampf, S.K., Burges, S.J.: Revised coefficients for priestley-taylor and makkink-hansen equations for estimating daily reference evapotranspiration. J. Hydrol. Eng. **18**(10), 1289–1300 (2013)
32. Kohler, M.A., Nordenson, T.J., Fox, W.E.: Evaporation from Pans and Lakes. US Government Printing Office, United States (1955)
33. McMahon, T.A., Peel, M.C., Lowe, L., Srikanthan, R., McVicar, T.R.: Estimating actual, potential, reference crop and pan evaporation using standard meteorological data: a pragmatic synthesis. Hydrol. Earth Syst. Sci. **17**(4), 1331–1363 (2013)
34. Hobbins, M.T., Ramirez, J.A., Brown, T.C.: The complementary relationship in estimation of regional evapotranspiration: an enhanced advection-aridity model. Water Resour. Res. **37**(5), 1389–1403 (2001)
35. Kim, H., Kaluarachchi, J.J.: Estimating evapotranspiration using the complementary relationship and the Budyko framework. J. Water Clim. Change **8**(4), 771–790 (2017)
36. Crago, R.D., Qualls, R.J., Feller, M.: A calibrated advection-aridity evaporation model requiring no humidity data. Water Resour. Res. **46**(9), 1–8 (2010)
37. Crago, R., Brutsaert, W.: A comparison of several evaporation equations. Water Resour. Res. **28**(3), 951–954 (1992)